Numerical Simulation Study on the Impact of Hydrogen Injection Quantities on Engine Performance and Emission Characteristics at Variable Speeds

Mahmoud Awaga^{1,□}, Nouby Ghazaly¹, Ahmad Omar², A.A Gomaa¹

Abstract— Hydrogen is a promising clean fuel for dualfuel diesel engines, aiming to enhance efficiency and reduce emissions. "This study employs ANSYS Forte simulations to investigate the impact of varying hydrogen injection ratios (15-70%) on engine performance and emissions at speeds between 1400 and 2500 RPM. At moderate enrichment levels (around 25%), Brake Thermal Efficiency (BTE) improves significantly, reaching ~45%, which represents a ~6% increase compared with conventional diesel baseline operation. Carbon-based emissions also decline sharply: CO and CO₂ are reduced by more than 40% relative to diesel-only cases, with CO₂ dropping to ~1.02E-04 g. Hydrogen further eliminates soot formation, addressing one of the major drawbacks of diesel However, combustion. these advantages counterbalanced by notable drawbacks: NOx emissions rise steeply at higher hydrogen shares, nearly doubling compared with the diesel baseline, and thermal efficiency decreases beyond 50% hydrogen due to excessive heat transfer losses and combustion instabilities. These tradeoffs highlight that while hydrogen enrichment enhances diesel engine sustainability, careful optimization of the hydrogen ratio and injection strategy is required to maximize efficiency and minimize NOx penalties. Further experimental validation is recommended to support the numerical findings and guide practical applications in clean transportation technologies. The study concludes that hydrogen can improve diesel engine sustainability, especially under strict emission standards. Balancing hydrogen ratios and injection timing is essential to maximize benefits while controlling NOx. Further experimental research is recommended to optimize system parameters and support clean transportation technologies.

Keywords: Alternative fuels; Dual-fuel diesel engine; (NOx) emissions; Brake thermal efficiency; Hydrogen enrichment.

Received: 19 June 2025/ Accepted: 02 November 2025

1 Introduction

The urgent necessity to reduce greenhouse gas emissions and decrease reliance on fossil fuels has driven significant research into alternative fuels for Compression Ignition (CI) engines in recent years [1]. While diesel engines are efficient, they emit particulate matter and nitrogen oxides (NOx), worsening air pollution and accelerating climate change [2]. Alternative fuels, such as natural gas, biodiesel, and methanol, offer the potential to mitigate these environmental impacts while maintaining performance [3]. Biodiesel, derived from vegetable or animal fats, is renewable, biodegradable, and produces fewer greenhouse gases over its lifecycle [4]. Although blends may slightly increase specific fuel consumption and lower thermal efficiency, transesterification reduces its viscosity, improving compatibility with diesel engines [5]. Biodiesel use significantly reduces particulate matter and unburned hydrocarbons, meeting strict environmental regulations, and further reduces greenhouse gas emissions relative to diesel [6]. Methanol is also under investigation due to its high-octane rating and favorable combustion characteristics. It can form stable blends with diesel, offering flexibility in fuel use and potential gains in efficiency with lower emissions [7]. Methanol's combustion in CI engines shows reduced NOx and higher thermal efficiency [8]. Advanced combustion technologies, such as homogeneous Charge Compression Ignition (HCCI) and reactivity-controlled Compression Ignition (RCCI), improve combustion control, lower pollutants, and enhance fuel efficiency [9]. Integrating alternative fuels with these systems can amplify environmental benefits without sacrificing performance, making their adoption essential for future energy and environmental targets [4].

Dual-fuel engines represent a key innovation, enabling simultaneous use of two fuels to optimize efficiency and emissions. They typically combine a gaseous primary fuel,

[□] Corresponding Author: Mahmoud Awaga, <u>fahdmasa@gmail.com</u>, Nouby Ghazaly, <u>nouby.ghazaly@eng.svu.edu.eg</u>, Ahmad Omar, <u>moaz777@eng.bsu.edu.eg</u>, A.A Gomaa, <u>a.a.gomaa@eng.svu.edu.eg</u>

^{1.} Mechanical Engineering Department, Faculty of Engineering, South Valley University, Qena 83523, Egypt

^{2.} Mechanical Engineering Department, Faculty of Engineering, Beni-Suef University, Egypt

like natural gas or biogas, with diesel as a pilot fuel. This configuration exploits diesel's ignition properties and gaseous fuels' cleaner combustion [10]. Combustion occurs via premixed and diffusion modes: gaseous fuel mixed with air is ignited by diesel injection at the end of the compression stroke [11] This approach improves combustion efficiency and significantly reduces NOx and particulate matter [12]. The flexibility to use fuels such as LNG and CNG makes dual-fuel systems attractive where gas availability or cost is favorable [13], and retrofitting existing diesel engines is feasible with moderate modifications [14].

Challenges remain, particularly under low load, where performance may drop due to the lower energy content of gaseous fuels and the complexity of combustion control [15]. Strategies like optimizing pilot injection timing and employing Exhaust Gas Recirculation (EGR) have been shown to mitigate these issues [16].

Hydrogen integration into dual-fuel engines is gaining attention to enhance both performance and sustainability [17]. Hydrogen, when used with diesel, benefits from its high flame speed, wide flammability range, and zero carbon content, eliminating CO2 and soot emissions [18-20]. It enables more complete fuel burns, reducing unburned hydrocarbons and NOx [17, 18], although under certain conditions it may raise CO emissions [21]. Hydrogen's high autoignition temperature necessitates a diesel pilot injection for ignition [22], where combustion is initiated at the end of the compression stroke. Optimizing pilot injection timing can improve pressure, combustion quality, and efficiency [23, 24], while EGR can lower combustion temperature and emissions [25]. However, hydrogen's high flame speed can cause pressure fluctuations and knocking, requiring careful control of its proportion in the mixture [23], [26].

Knock suppression in hydrogen-diesel dual-fuel engines can be achieved through optimized injection strategies. Adjusting timing and pilot fuel quantity significantly affects combustion and knock intensity. Lowering compression ratios, as demonstrated by reducing from 16.5:1 to 15.5:1, decreases in-cylinder temperatures, reducing both knocking and NOx emissions [27]. EGR is another effective measure, lowering combustion temperatures and enhancing knock resistance [28, 29].

Hydrogen's unique physical and chemical properties shown in **Table 1** distinguish it from common transport fuels like CNG, gasoline, and diesel [30]. Its zero-carbon content means NOx is the sole harmful combustion product, as CO, CO₂, and soot are eliminated. With a high specific energy density, hydrogen can deliver nearly triple the energy per unit mass compared to fossil fuels, despite its lower heating value [31]. These attributes, combined with ongoing advances in engine design, position hydrogen as a leading candidate in the transition to clean, efficient internal combustion technologies.

Table 1 Hydrogen properties compared with methane, gasoline and diesel [32]

Properties	Hydrogen	Methane	Gasoline	Diesel
Molecular weight (g/mol)	2.016	16.043	107	107
Density(kg/m³)	0.08	0.65	750	840
Mass diffusivity in air (cm ² /s)	0.61	0.16	-	-
Flammability limits in air (vol%)	4-75	5-15	1-7.6	0.7-7.5
Burning velocity (m/s)	2.65-3.25	0.37-0.43	0.45	0.3
Quenching distance (mm)	0.61	2.00	2.00	-
Autoignition temperature (K)	858	813	523	483
Minimum ignition energy (mJ)	0.02	0.28	0.24	0.24
Adiabatic flame temperature (K)	2390	2226	2275	2275
Stoichiometric air/fuel ratio by mass	34.3	17.2	14.5	14.5
Lower heating value (MJ/kg)	120	50	43.4	42.6

2 Numerical Methodology and Modelling Setup

ANSYS Forte is a Computational Fluid Dynamics (CFD) tool specifically designed for simulating internal combustion engines, including dual-fuel engines that utilize both diesel and hydrogen. In this context, the software is employed to model complex fluid dynamics, combustion processes, and emissions formation within the engine. The numerical methods and models used in ANSYS Forte provide insights into the performance, efficiency, and environmental impact of dual-fuel systems. This section outlines the key numerical models and methodologies employed in ANSYS Forte for dual-fuel engine simulations.

2.1 Governing Equations

The simulation of dual-fuel engines in ANSYS Forte is governed by the fundamental fluid dynamics equations: Navier-Stokes Equations: These equations describe the motion of the fluid (air-fuel mixture) within the engine. They account for mass, momentum, and energy conservation, which are critical for modeling the behavior of the fuel and air as they mix and combust [32].

$$\frac{\partial \rho}{\partial t} + \frac{\partial \rho \bar{u}_j}{\partial x_i} = S_m \tag{1}$$

Momentum:

Mass:

$$\frac{\partial \rho \bar{u}_{i}}{\partial t} + \frac{\partial \rho \bar{u}_{i} \bar{u}_{j}}{\partial x_{j}} = -\frac{\partial \bar{P}}{\partial x_{i}} + \frac{\partial}{\partial x_{j}} \left(\mu \left(\frac{\partial \bar{u}_{j}}{\partial x_{i}} + \frac{\partial \bar{u}_{i}}{\partial x_{j}} - \frac{2}{3} \delta_{ij} \frac{\partial \bar{u}_{k}}{\partial x_{k}} \right) \right) - \frac{\partial \rho \bar{u}'_{i} u'_{j}}{\partial x_{i}} + S_{i} \tag{2}$$

Energy:

$$\frac{\partial \rho \bar{H}}{\partial t} + \frac{\partial \rho \bar{u}_j \bar{H}}{\partial x_j} = \frac{\partial}{\partial x_j} \left(\frac{k_{eff}}{C_p} \frac{\partial \bar{H}}{\partial x_j} \right) + S_h \tag{3}$$

Species:

$$\frac{\partial \rho \bar{Y}_n}{\partial t} + \frac{\partial \rho \bar{u}_i \bar{Y}_n}{\partial x_i} = -\frac{\partial J_n}{\partial x_i} + R_n + S_n \tag{4}$$

Three further transport equations for pollutant emissions are solved post-time step for computational efficiency. NOx emissions are calculated using the following transport equation for the NOx mass fraction, \bar{Y}_{NO_x} , accounting for thermal and prompt mechanisms

$$\frac{\partial \rho \bar{Y}_{NO_x}}{\partial t} + \frac{\partial \rho \bar{u}_j \bar{Y}_{NO_x}}{\partial x_j} = \frac{\partial}{\partial x_j} \left(\rho D \frac{\partial \bar{Y}_{NO_x}}{\partial x_j} \right) + S_{NO_x}$$
 (5)

Soot emissions are calculated using the Moss-Brookes soot model using acetylene as the inception species. Two additional transport equations are solved for the soot mass fraction, \bar{Y}_{soot} , given by:

$$\frac{\partial \rho \bar{Y}_{\text{soot}}}{\partial t} + \frac{\partial \rho \bar{u}_j \bar{Y}_{\text{soot}}}{\partial x_j} = \frac{\partial}{\partial x_j} \left(\frac{\mu_t}{\sigma_{\text{soot}}} \frac{\partial \bar{Y}_{\text{soot}}}{\partial x_j} \right) + \frac{dM}{dt}$$
 (6)

and the normalized radical nuclei concentration \bar{b}^*_{nuc}

$$\frac{\partial \rho \overline{b^*}_{nuc}}{\partial t} + \frac{\partial \rho \overline{u}_j \overline{b^*}_{nuc}}{\partial x_i} = \frac{\partial}{\partial x_i} \left(\frac{\mu_t}{\sigma_{nuc}} \frac{\partial \overline{b^*}_{nuc}}{\partial x_i} \right) + \frac{1}{N_{\text{norm}}^*} \frac{dN^*}{dt}$$
(7)

where ρ is the density of the fluid, t is time, \bar{u}_i a component of the mean velocity vector, u'_i a component of the fluctuating velocity vector, x_j a component of the position vector, S_m the source term accounting for mass added by fuel spray, P is pressure, μ is molecular viscosity, S_i a component of the body forces, d_{ij} the Kronecker delta, \bar{H} the mean total enthalpy, k_{eff} the effective conductivity, C_p the specific heat capacity of the fluid, S_h the source term accounting for any further heat losses, \bar{Y}_n is the mass fraction of species n, J_n is the diffusion flux of the given species, R_n the net rate of production of the given species by chemical reaction, S_n the rate of creation of the species by the discrete phase injection and any other sources, D is the effective diffusion coefficient, S_{NO} is the source term for any other NO_x production due to thermal or prompt mechanisms, μ_t is the turbulent viscosity, $\sigma_{\rm soot}$ is the turbulent Prandtl number for soot transport, M is the soot mass concentration, σ_{nuc} is the turbulent Prandtl number for radical nuclei transport, N^* is the soot particle number density and N^*_{norm} is 10^{15} particles [32].

2.2 Model validation

In this section Yasin Karagöz [23], experimentally investigated the use of hydrogen as an additive gaseous fuel introduced into the intake manifold through gas injectors, while diesel fuel was injected into the cylinder using a diesel injector and served as the ignition source. Energy content of introduced hydrogen was set to 0%, 25% and 50% of total fuel energy, where the 0% references neat diesel operation without hydrogen injection. conditions were set to full load at 750, 900, 1100, 1400, 1750 and finally 2100 r/min engine speed. Variation in emissions performance. and combustion characteristics with the effect of hydrogen addition was investigated, as shown in Fig. 1 and Fig. 2.

The study evaluated hydrogen—diesel dual-fuel operation in a single-cylinder, four-stroke diesel engine by introducing hydrogen at 25% and 50% of the total fuel energy, with diesel serving as the igniter. **Figure. 3** shows hydrogen addition improved carbon-based emissions, reducing CO by 20.4–66.3%, CO₂ by 12.7–38.7%, and smoke by 10.4–58.2% due to more homogeneous combustion. However, NO_x emissions increased by 15.2–212.7%, and engine performance suffered, with brake power and thermal efficiency dropping by 8.1–25.4% and 3.3–15.5%, respectively, primarily from decreased volumetric efficiency.

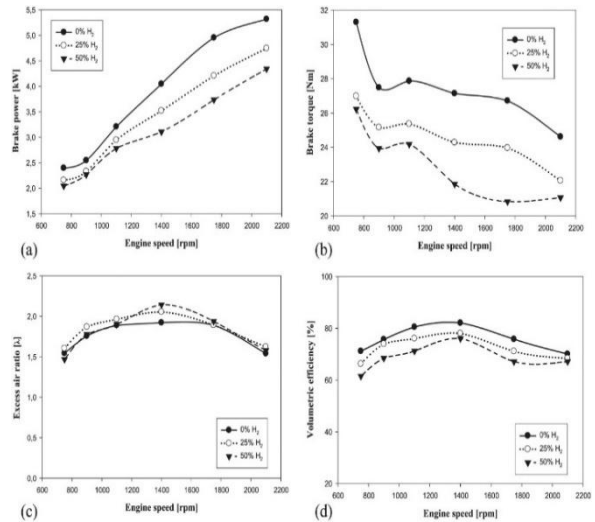


Fig. 1 (a) Brake power, (b) Brake torque, (c) Excess air ratio (d) volumetric efficiency based on the rate of hydrogen

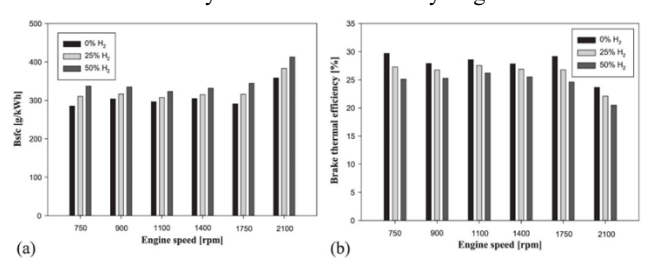


Fig. 2 Based on engine speed, the brake-specific fuel consumption value variation (a) and brake thermal efficiency value variation (b) at varied hydrogen levels

In this work, the authors based their validation on the experimental study by Faghani [33] which investigated a dual direct-injection diesel-natural gas engine. Since experimental data for diesel-hydrogen dual direct injection is scarce, the natural gas case was chosen as a suitable reference, supported by the inclusion of a detailed hydrogen oxidation mechanism in the chemical model.

A sector geometry representing one-seventh of the combustion chamber (due to seven diesel and seven gas injectors) was created to reduce computational cost. Appropriate thermal boundary conditions (600 K for the head and 650 K for the piston bowl) were applied, and the initial charge properties, including EGR level, pressure, and temperature, were matched to the experimental values.

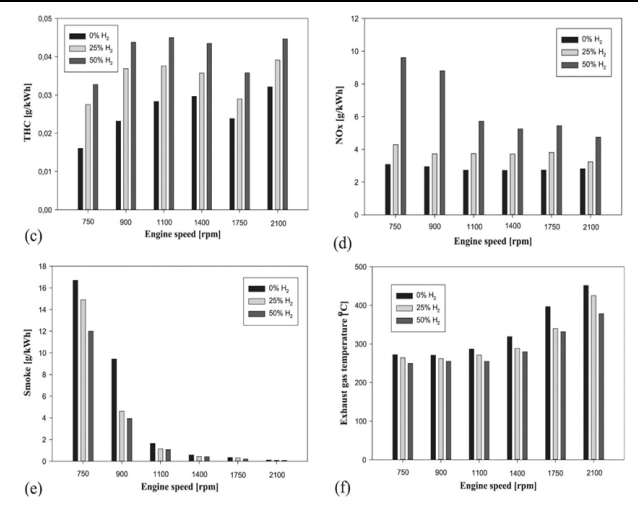


Fig. 3 (a) Changes in the value of CO emissions, (b) Variability in CO₂ emission value, (c) Changes in THC emission levels, (d) Changes in NOx emission values, (e) Changes in smoke emission values and (f) Variations in the temperature of exhaust gas depending

Figure 4 shows mesh sensitivity study was then carried out using four grid resolutions (coarse, medium, fine, very fine). As can be seen in **Fig. 5**, the coarse mesh underpredicted combustion rate and delayed ignition, while the medium and fine meshes closely matched the measured in-cylinder pressure and Heat Release Rate (HRR). Differences between the fine (0.35 mm) and very fine (0.3 mm) meshes were negligible, so the fine mesh was adopted for all subsequent simulations, striking a balance between accuracy and computational time.

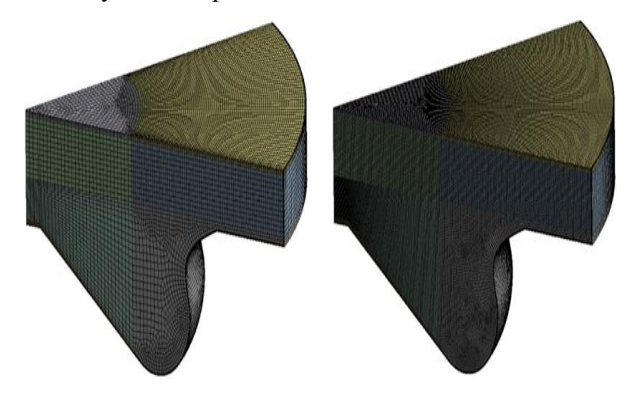


Fig. 4 Sector mesh at 700°CA used in combustion simulations. Left shows the "coarse" grid used to compute the compression stroke prior to injection and right shows the "fine" key grid, with a maximum mesh size of 0.35 mm, used during injection and combustion

Validation also covered pollutant emission trends shown in **Fig. 6**. CFD predictions of NOx and soot under varying EGR rates reproduced the experimental trends: NOx decreased by 82% in simulations (80% in experiments), while soot increased as expected, although the absolute soot levels were underpredicted. This confirmed that the model could reliably capture the main physical and chemical trends.

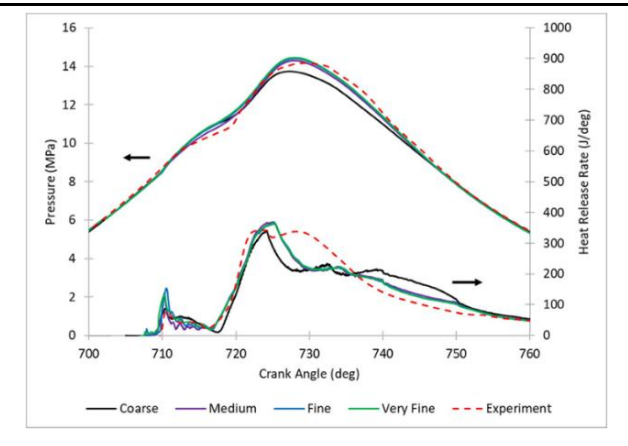


Fig. 5 Pressure and heat release rate predictions and mesh sensitivity study for the 18% EGR test case with comparison to experimental data

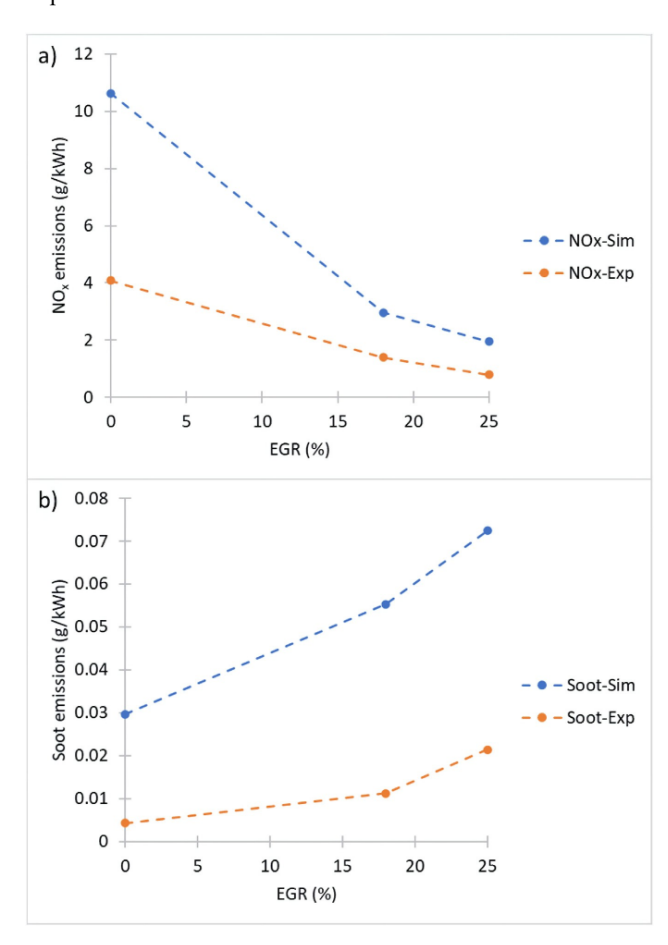


Fig. 6 Pollutant trend predictions of a) NOx and b) Soot at EVO for increasing levels of EGR compared with experimental measurement

The validation framework combined (1) comparison with experimental combustion data, (2) mesh independence analysis, and (3) reproduction of pollutant trends. These steps established confidence that the CFD setup could be applied to study diesel-hydrogen dual direct injection with sufficient accuracy. Although the CFD simulations

successfully reproduced the overall experimental trends for combustion and emissions, some quantitative deviations, particularly in soot predictions, highlight inherent model limitations. Future work should therefore include a broader uncertainty assessment to enhance the robustness and credibility of the results.

2.3 Methods and materials

The primary goal of this study is to investigate the use of hydrogen in dual fuel diesel engines to enhance engine efficiency and reduce Carbon Monoxide (CO) emissions.

The hypothesis is that by increasing the proportion of hydrogen in the fuel mixture, engine efficiency will improve, and pollutant emissions will decrease. The experiments were conducted using ANSYS Forte, a specialized software for simulating combustion processes in internal combustion engines. A computational model was developed to simulate the performance of a dual-fuel diesel engine operating with varying percentages of hydrogen with RPM varying. The sector model approach was employed, focusing on a 60-degree section of the combustion chamber as shown in **Fig. 7**.

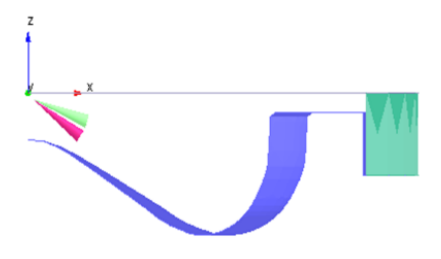


Fig. 7 Sector angle for model simulation.

A 60-degree sector model of the diesel engine combustion chamber was designed in ANSYS Forte. This sector was chosen for computational efficiency while maintaining accuracy in the analysis. The model used two fuel injectors for direct injection of both diesel and hydrogen. Piston temperature 600 K, head temperature 650 K, initial temperature is 362 K and initial pressure 2.215 bar. **Table 2** shows summary of engine parameters.

Table 2 Summary of engine parameters

Item	Value
Engine Bore [cm]	13.72
Geometric Compression Ratio	16.12108
Total Fuel Mass [g]	6.70E-02
Pilot start of injection (CA)	703 BTDC
H2 start of injection (CA)	712 BTDC
Cone Angle	12°

This study focuses on the use of hydrogen as a dual fuel in a diesel engine, aiming to improve engine efficiency and reduce CO emissions. The research is based on computational simulations using ANSYS Forte, a powerful engine simulation software. The study investigates how varying the percentage of hydrogen injected into the engine affects its performance across different RPMs. The study's protocol outlines how the simulations were conducted, the variables used, and the data analyzed. The study begins by examining the engine's performance at a base speed of 1400 RPM. This speed was selected as a starting point because it represents a common operating speed for medium-load conditions in diesel engines. By choosing 1400 RPM, the study captures data relevant to the typical working range of diesel engines, particularly in applications such as commercial vehicles and generators. Once the engine's behavior at 1400 RPM was analyzed, further simulations were conducted at higher RPMs: 1800, 2000, and 2500 RPM. These additional RPMs represent a broader range of operating conditions. For instance, 1800 RPM corresponds to low to medium load conditions, while 2000 RPM and 2500 RPM simulate high-speed engine operations. By simulating across this range, the study covers a comprehensive performance spectrum, ensuring that both low and high-speed efficiency and emissions characteristics are captured. Each RPM setting was subjected to five different hydrogen-to-total fuel ratios, which ensured that the effect of increasing hydrogen concentration on performance and emissions could be thoroughly studied under different load conditions.

Hydrogen was injected into the engine in five varying concentrations relative to the total fuel mass. The hydrogen-to-total fuel mass percentages were set at 15%, 25%, 50%, 60%, and 70%. The following considerations informed the selection of these specific percentages:

Low Hydrogen Concentrations (15% and 25%): These levels were chosen to examine the impact of minor hydrogen additions on combustion characteristics. Low hydrogen concentrations allow for a relatively gradual introduction of the more reactive hydrogen into the combustion process, providing insight into how the engine responds with minimal hydrogen addition.

Moderate Hydrogen Concentration (50%): This represents a balanced mixture of hydrogen and diesel, with hydrogen making up half of the total fuel mass. This ratio is critical for understanding the engine's transitional behavior as hydrogen moves from being a secondary fuel to sharing equal prominence with diesel in the combustion process.

High Hydrogen Concentrations (60% and 70%): These levels were chosen to assess the upper limits of hydrogen usage in the dual-fuel system. Since hydrogen burns faster and at higher temperatures than diesel, it's important to evaluate how the engine manages combustion stability, knock, and thermal efficiency when hydrogen dominates the fuel mixture. Each of these hydrogen concentration levels was applied consistently across the RPM range, allowing for direct comparison between the engine's response to hydrogen at different speeds. The engine simulation model used two separate injectors for hydrogen and diesel, both employing direct injections to introduce the fuels into the combustion chamber:

Hydrogen Injector: The hydrogen was injected at an angle of 712 degrees in the engine cycle. This specific angle was selected based on its alignment with the ideal timing for hydrogen combustion, ensuring that hydrogen is introduced at the point in the cycle where the in-cylinder conditions (pressure and temperature) are optimal for complete combustion.

Diesel Injector: The diesel fuel was injected at 703 degrees, slightly earlier than hydrogen. The diesel's earlier injection allows it to serve as a pilot fuel, igniting first and providing the necessary heat to initiate the combustion of hydrogen. This sequential injection strategy ensures stable combustion, particularly at high hydrogen concentrations, where premature ignition or knock could otherwise occur. The total mass of fuel injected in each simulation cycle was kept constant at 0.067 grams. This constant fuel mass ensured that the only variable difference between simulations was the hydrogen-to-diesel ratio, allowing for a controlled comparison across different hydrogen percentages and RPM settings.

During each simulation, various performance and emission parameters were closely monitored. These included:

Brake Thermal Efficiency (BTE): BTE measures how efficiently the engine converts fuel into mechanical work. The study tracked how increasing the proportion of hydrogen affected the engine's overall efficiency. Hydrogen's higher energy content, compared to diesel, was expected to improve BTE at higher injection levels, particularly under medium to high load conditions.

In-Cylinder Pressure and Temperature: The combustion process was monitored for peak in-cylinder pressure and temperature. Higher hydrogen concentrations were expected to result in sharper pressure peaks due to hydrogen's faster burn rate. Understanding how these peaks varied with RPM was critical to assessing the engine's mechanical durability and combustion stability.

Emissions: Emission analysis was a key component of the study. Carbon monoxide (CO), nitrogen oxides (NOx), and unburned hydrocarbons (UHC) were measured for each hydrogen-diesel combination. The hypothesis was that higher hydrogen concentrations would significantly reduce CO emissions, given hydrogen's carbon-free nature. However, the potential increase in NOx due to higher combustion temperatures was also a concern. The study tracked NOx emissions to ensure that any improvements in CO emissions did not come at the expense of increased NOx production. Knock, a phenomenon where fuel-air mixtures ignite prematurely, was a major focus of the study, especially at higher hydrogen concentrations. Since hydrogen has a lower ignition energy and higher flame speed than diesel, it increases the likelihood of knocking under certain conditions. The simulations monitored the occurrence of knock and sought to understand how hydrogen percentages and RPM affected its prevalence.

By injecting diesel slightly earlier than hydrogen, the study aimed to use diesel as a stabilizing influence, igniting first and controlling the overall combustion process. This strategy was expected to minimize knock risk, particularly at high hydrogen concentrations.

For each combination of RPM and hydrogen percentage, detailed data was collected on engine performance and emissions. This data was analyzed to: Establish trends in efficiency gains or losses as hydrogen concentration increased.

Identify optimal hydrogen percentages for reducing CO emissions while maintaining engine stability and avoiding excessive NOx production. Evaluate how engine load (as represented by RPM) interacted with hydrogen concentration to affect overall performance. "In this work, Brake Thermal Efficiency (BTE) denotes the ratio of brake power to total fuel energy. Thermal efficiency reflects the ideal fuel-to-work conversion, while combustion efficiency indicates the completeness of fuel burning. These distinctions clarify performance evaluation and avoid confusion when interpreting simulation results."

3 Results and Discussion

3.1 Case A at 1400 RPM

In Case A, the engine's performance was evaluated at a constant speed of 1400 RPM with varying hydrogen injection percentages of 15%, 25%, 50%, 60%, and 70% of the total fuel mass. The results were visualized using simulation diagrams and pictures obtained from the ANSYS Forte model, which was specifically designed and calibrated by ANSYS to match the specifications of the studied engine. This ensured that the outcomes accurately reflected the engine's real operational behavior under different hydrogen concentrations.

Figure 8 clearly shows the strong hydrogen enrichment effect. strongly improves combustion but alters emission trends. CO and soot decrease sharply, nearly disappearing at 60–70% due to faster oxidation and hydrogen's carbonfree nature. CO₂ is higher at 15–25% H₂ from diesel dominance but falls at higher shares as less carbon is present. H₂ is partly unburned at 15%, yet higher ratios ensure better mixing and complete consumption. However, NOx rises notably with hydrogen, especially at 50–70%, linked to elevated temperature fields exceeding 2000 K. Pressure also increases, reflecting greater heat release.

The results demonstrate clear effects of hydrogen enrichment on engine performance and emissions in Fig. 9. Total chemical heat release increases steadily with hydrogen share, reflecting the high heating value and fast reactivity of hydrogen. In Fig. 10, combustion efficiency rises above 97% at moderate ratios, though it is lower at 15% H₂ due to incomplete combustion. Gross ISFC decreases significantly, showing better fuel utilization. Thermal efficiency peaks at 25–50% H₂ but declines at 70%

because of higher heat losses and NOx formation. Maximum temperature increases with hydrogen, explaining the strong growth of EINOx emissions, which nearly double from 15% to 70%.

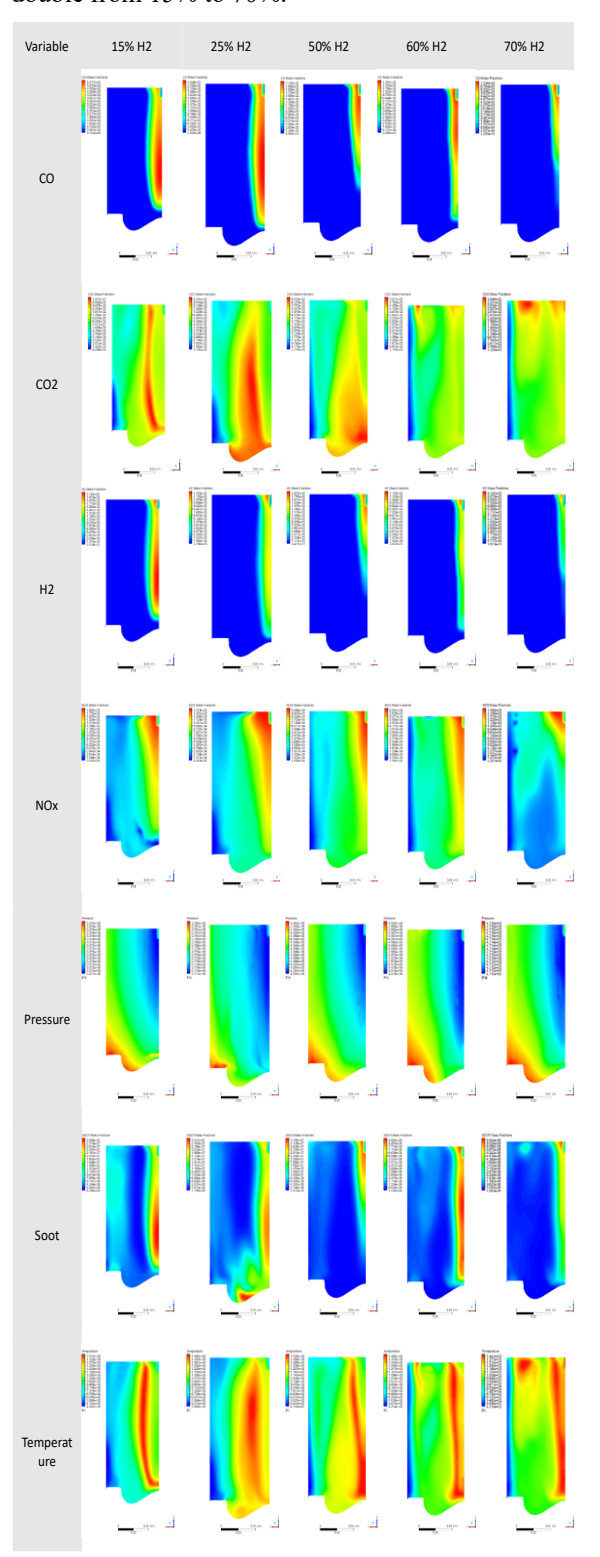


Fig. 8 Contours of CO, CO₂, H₂, N₂, NO, NO₂, NOx, Pressure, Soot and temperature at 1400 RPM

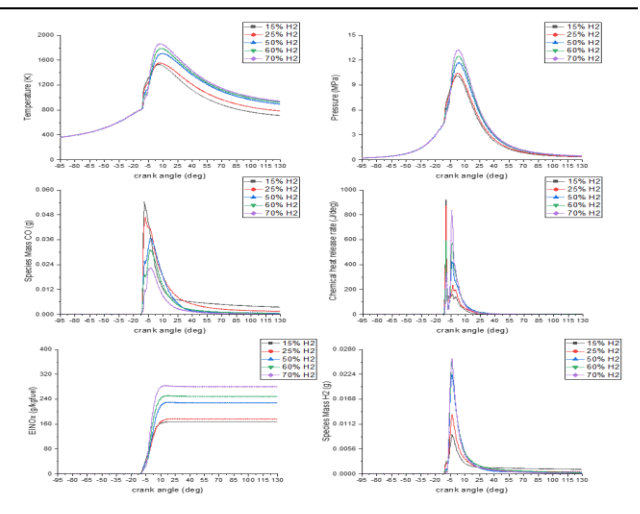


Fig. 9 Calculated temperature, pressure, chemical heat release rate, speciesmass CO, speciesmass of H2 and EINOx at 1400 RPM



Fig. 10 Calculated total chemical heat release, Combustion Efficiency, Gross ISFC, thermal efficiency, maximum temperature, EINOX, CO, and soot at Hydrogen energy share at 15%, 25%, 50%, 60%, 70% at 1400 RPM

Emission trends are also notable: CO emissions drop sharply with hydrogen, from 3.49E-03 g to nearly negligible at 70% H₂, due to improved oxidation. Similarly, soot emissions decline drastically because hydrogen is carbon-free and enhances cleaner burning. Overall, moderate hydrogen levels (25–50%) achieve the best compromise between efficiency improvements and emission control.

3.2 Case B at 1800 RPM

In Case B, the engine's performance was evaluated at a constant speed of 1800 RPM with varying hydrogen injection percentages of 15%, 25%, 50%, 60%, and 70% of the total fuel mass.

In **Fig. 11**, the effect of hydrogen enrichment on engine performance and emissions is clearly demonstrated. as we can see **Fig. 12** the Total chemical heat release rises continuously from 3614 J at 15% H₂ to 6408 J at 70% H₂, reflecting hydrogen's higher reactivity and calorific value. Similarly, combustion efficiency improves from 93.6% to nearly 97.9% at 25–50% H₂, before stabilizing, showing more complete oxidation at moderate blends.

Fuel utilization also improves, as shown in **Fig. 13** by the drop in gross ISFC from 141.36 g/kWh at 15% H₂ to 86.17 g/kWh at 70% H₂. Thermal efficiency, however, peaks at 45.5% around 15–25% H₂ and gradually decreases to 42.6% at 70%, likely due to higher heat losses and NOxrelated penalties at extreme enrichment.

As expected, maximum temperature increases with hydrogen share, exceeding 1800 K at 60–70% H₂. This correlates directly with the sharp rise in EINOx, which nearly doubles from ~1.0E-2 g to 1.96E-2 g, indicating a significant environmental drawback.

On the positive side, CO emissions are reduced drastically, falling from 3.33E-03 g to almost negligible levels at 70% H₂. Soot emissions also decrease markedly because hydrogen is carbon-free and promotes cleaner combustion.

3.3 Case C at 2000 RPM

In Case C, the engine's performance was evaluated at a constant speed of 2000 RPM with varying hydrogen injection percentages of 15%, 25%, 50%, 60%, and 70% of the total fuel mass.

Figure 14 shows the contours of the analysis at 2000 RPM, hydrogen enrichment strongly affects both performance and emissions, and **Fig. 15** shows the graphs of the total chemical heat release rises from 3644 J at 15% H₂ to 6412 J at 70% H₂, reflecting hydrogen's high reactivity. Combustion efficiency also improves, reaching nearly 97.9% at 50–60% H₂, compared with only 97.2% at 15% H₂.

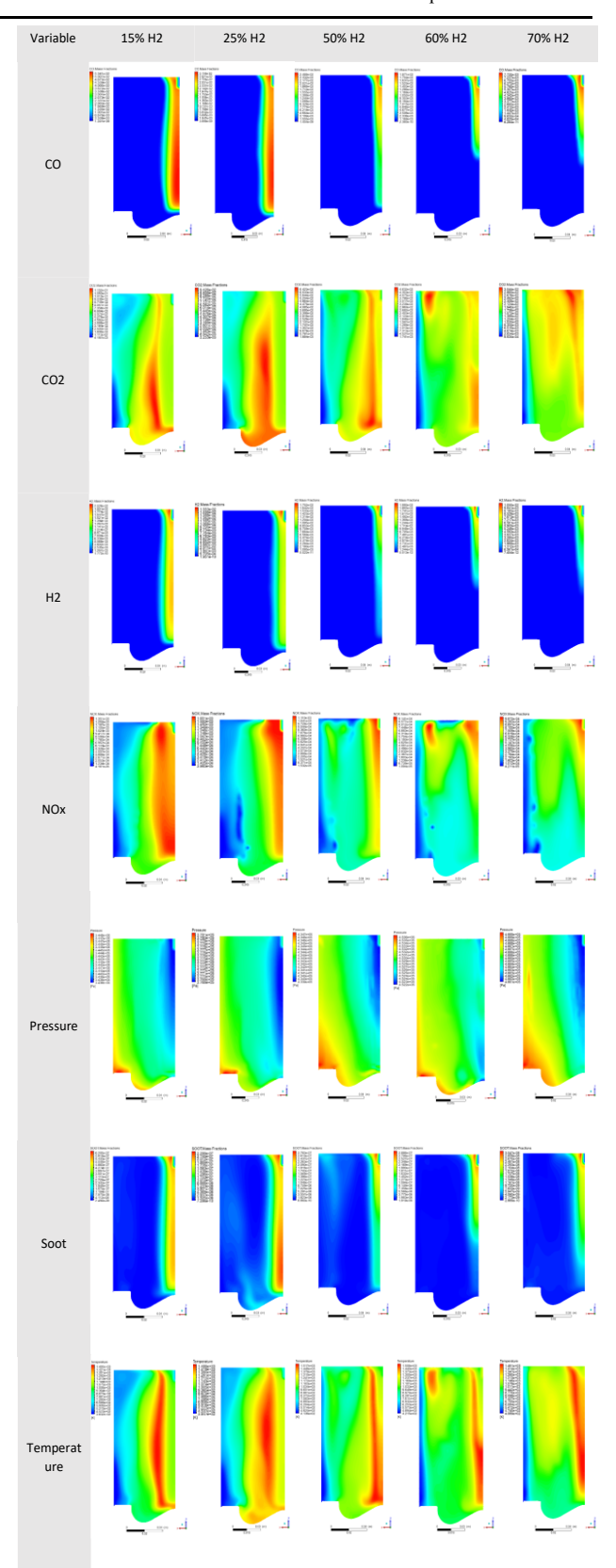


Fig. 11 Contours of CO, CO₂, H₂, N₂, NO, NO₂, NOx, Pressure, Soot and temperature at 1800 RPM

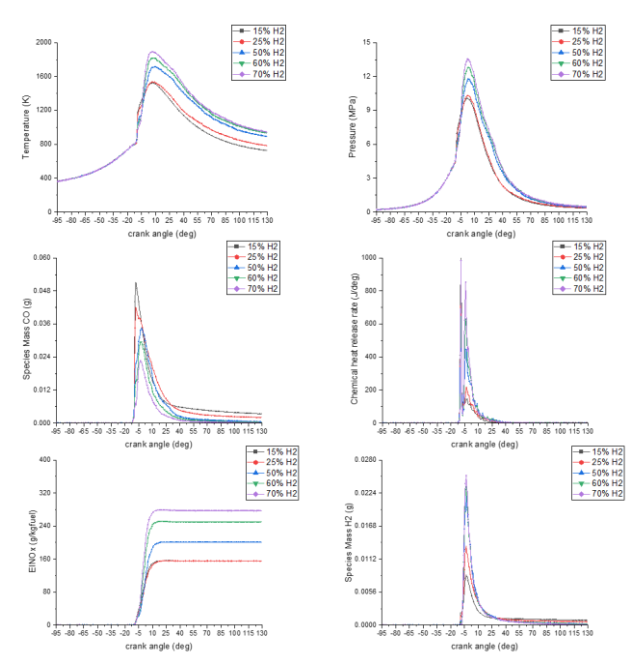


Fig. 12 Calculated temperature, pressure, chemical heat release rate, speciesmass CO, speciesmass of $\rm H_2$ and EINOx at 1800 RPM



Fig. 13 Calculated total chemical heat release, Combustion Efficiency, Gross ISFC, thermal efficiency, maximum temperature, EINOX, CO, and soot at Hydrogen energy share at 15%, 25%, 50%, 60%, 70% at 1800 RPM

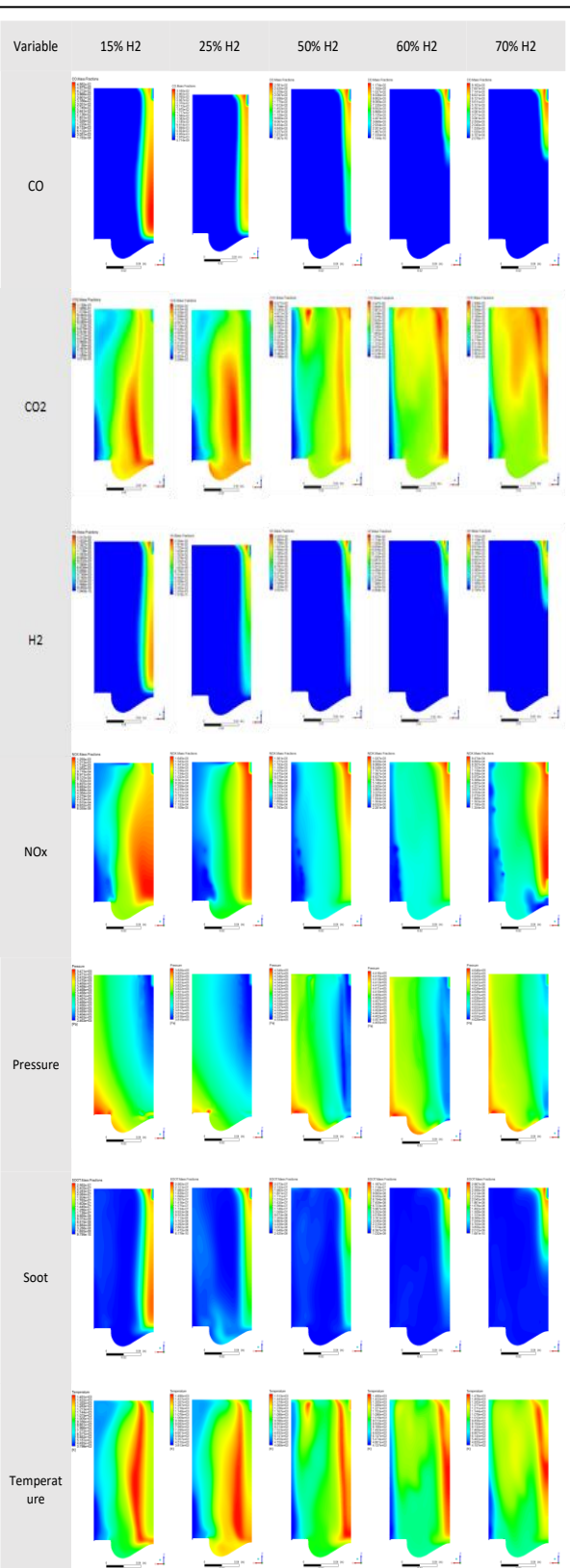


Fig. 14 Contours of CO, CO₂, H_2 , N_2 , NO, NO_2 , NOx, Pressure Soot and temperature at 2000 RPM

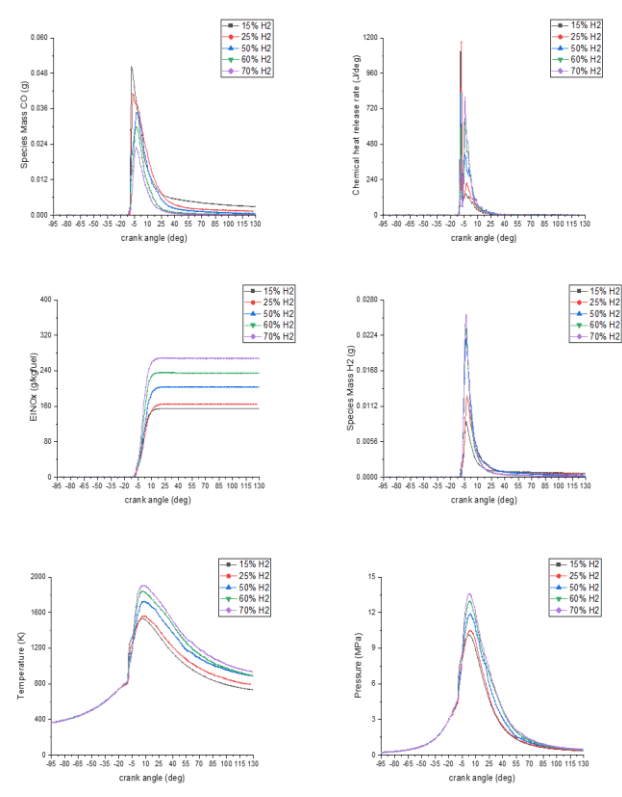


Fig. 15 Calculated temperature, pressure, chemical heat release rate, speciesmass CO, speciesmass of H₂ and EINO at 2000 RPM

Figure 16 illustrates the benefits of fuel utilization. Benefits are evident from the reduction in gross ISFC, decreasing from 139.5 g/kWh to 85.8 g/kWh as hydrogen share increases. Thermal efficiency, however, shows a peak of 46.25% at 25% H₂ before gradually declining to 42.8% at 70% H₂, suggesting that excessive enrichment increases heat losses and reduces net efficiency.

The maximum temperature rises steadily, exceeding 1900 K at high hydrogen ratios. This explains the growth in EINOx, which increases from 1.0E-2~g at $15\%~H_2$ to 1.8E-2~g at $70\%~H_2$.

On the other hand, carbon-related pollutants are sharply reduced. CO emissions fall from 2.83E-03 g to near zero at 70% H₂, and soot emissions also decrease dramatically due to hydrogen's carbon-free nature and faster oxidation.

3.4 Case D at 2500 RPM

In Case D, the engine's performance was evaluated at a constant speed of 2500 RPM with varying hydrogen injection percentages of 15%, 25%, 50%, 60%, and 70% of the total fuel mass.

Figure 17 shows the contours of the analysis at 2500 RPM, it is observed that combustion efficiency reaches its peak with a hydrogen blending rate of 70%. This demonstrates that the introduction of a high proportion of hydrogen into the fuel mix can significantly enhance the combustion process, allowing for more complete fuel utilization. The

total chemical heat release, which reflects the amount of energy released during combustion, also remains highest at this 70% hydrogen level. This confirms that, in terms of energy potential, a higher hydrogen concentration leads to greater heat generation within the combustion chamber.

However, when examining thermal efficiency in **Fig. 18**, a different trend emerges. Despite the increased combustion efficiency at 70% hydrogen, the highest thermal efficiency is observed at a much lower hydrogen blend of 25%. This discrepancy highlights the fact that while more energy is released at higher hydrogen concentrations, not all of it is effectively converted into useful work. In fact, the thermal efficiency at 70% hydrogen is significantly lower compared to the 25% hydrogen blend. This suggests that, beyond a certain point, the additional heat generated at high hydrogen concentrations may result in greater energy losses, such as heat dissipation or incomplete energy conversion.



Fig. 16 Calculated total chemical heat release, Combustion Efficiency, Gross ISFC, thermal efficiency, maximum temperature, EINOx, CO, and soot at Hydrogen energy share at 15%, 25%, 50%, 60%, 70% at 2000 RPM

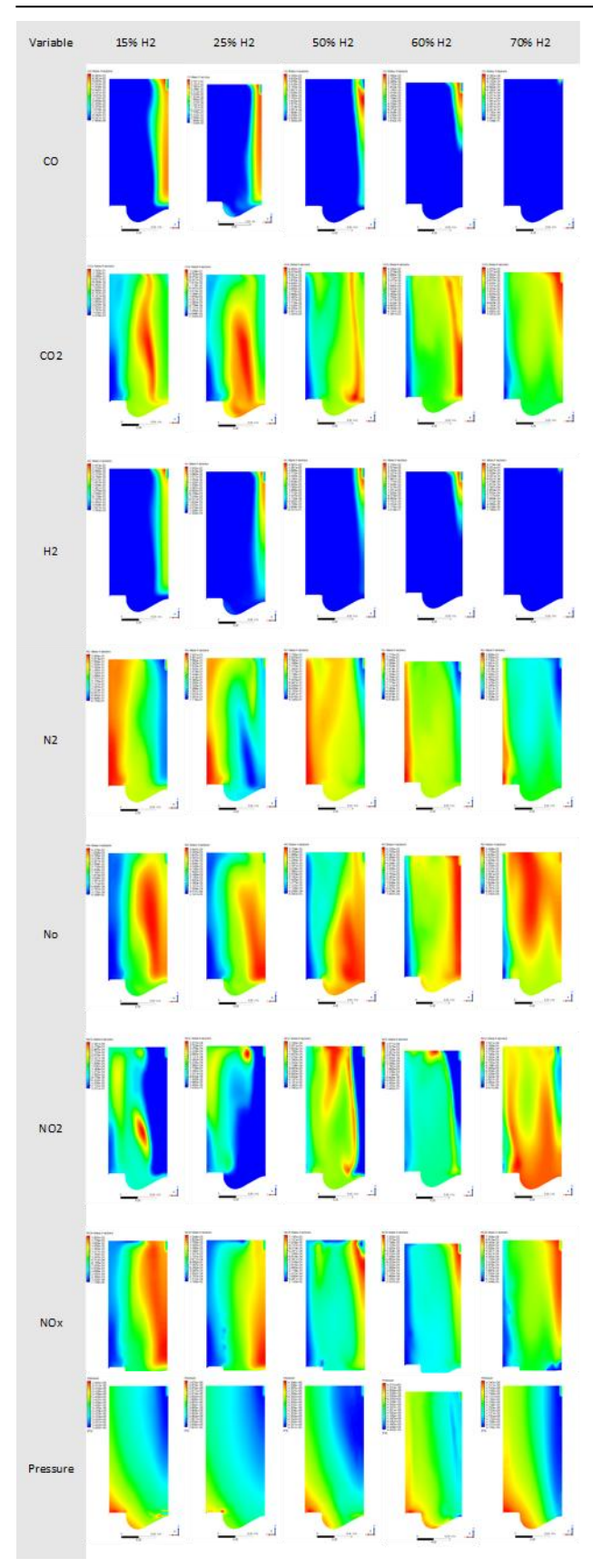


Fig. 17 Contours of CO, Co₂, H₂, N₂, NO, NO₂, NOx, Pressure, Soot and temperature at 2500 RPM

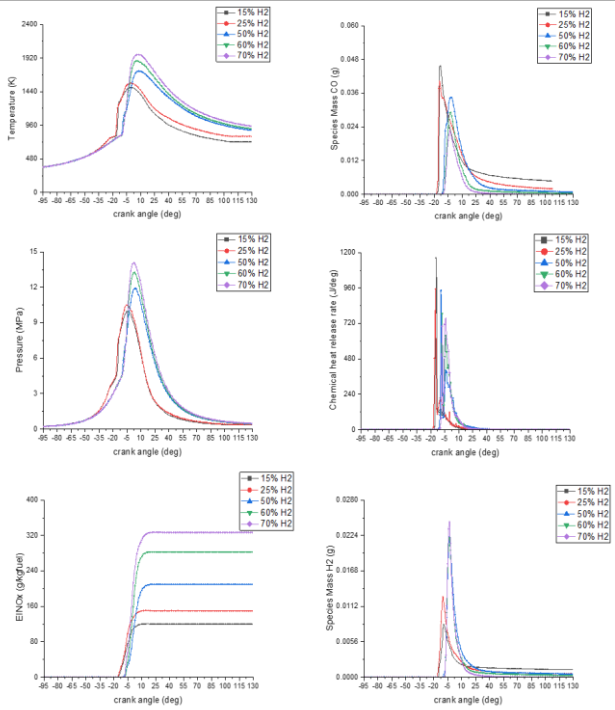


Fig. 18 Calculated temperature, pressure, chemical heat release rate, speciesmass CO, speciesmass of H₂ and EINOx at 2500 RPM

The low thermal efficiency at 70% hydrogen is a critical finding that is shown in **Fig. 19** because thermal efficiency measures how well the engine converts the chemical energy of the fuel into mechanical energy. A reduction in thermal efficiency, despite a high combustion efficiency, indicates that the system is not optimizing the available energy for useful work. Therefore, even though 70% of hydrogen provides the highest combustion efficiency, it is not an ideal condition for practical engine performance, as thermal efficiency becomes too low to support efficient combustion.

In terms of emissions, the highest levels of EINOx (Nitrogen Oxide Emissions Index) are recorded at 70% hydrogen. This is expected due to the elevated combustion temperatures associated with higher hydrogen concentrations. NOx emissions typically increase with higher temperatures because nitrogen in the air reacts more readily under these conditions, forming nitrogen oxides. Conversely, the lowest EINOx levels occur at 15% hydrogen, where the lower combustion temperature leads to a decrease in NOx formation.

Soot emissions, on the other hand, are minimal at 70% hydrogen. Hydrogen, being a clean-burning fuel, does not produce carbon-based soot like traditional hydrocarbon fuels. This results in significantly lower soot emissions as hydrogen concentration increases, particularly at higher blends like 70%.

The highest combustion temperatures are also observed at 70% hydrogen, due to hydrogen's fast flame speed and higher energy density. While this increases combustion efficiency, it also contributes to the rise in NOx emissions and can lead to thermal stress on engine components.



Fig. 19 Calculated total chemical heat release, Combustion Efficiency, Gross ISFC, thermal efficiency, maximum temperature, EINOx, CO, and soot at Hydrogen energy share at 15%, 25%, 50%, 60%, 70% at 2500 RPM

At hydrogen enrichment levels beyond 50%, the Brake Thermal Efficiency (BTE) begins to decline despite higher combustion efficiency. This reduction is mainly due to hydrogen's very high flame speed, which causes sharp pressure rises and elevated in-cylinder temperatures, leading to greater heat transfer losses to the cylinder walls rather than conversion into useful work. At the same time, these higher temperatures intensify NOx formation through the thermal Zeldovich mechanism, where nitrogen and oxygen react more readily under such conditions. Consequently, while moderate hydrogen ratios improve performance, excessive enrichment increases thermal losses and exacerbates NOx emissions, limiting overall efficiency.

7 Conclusion

The findings across different engine speeds (1400 to 2500 RPM) highlight the complex relationship between hydrogen injection levels, combustion efficiency, and emissions. While increasing hydrogen injection improves certain combustion characteristics, it does not result in a

simple, linear improvement in thermal efficiency. At low hydrogen injection levels, such as 15%, emissions like Nitrogen Oxides (NOx) remain low about 1.1E-02 g at 15%, but combustion efficiency and fuel performance are suboptimal about 97%.

As the hydrogen ratio increases, particularly at 50% and beyond, combustion efficiency improves significantly, leading to cleaner combustion with lower Carbon Monoxide (CO) and soot emissions. However, higher hydrogen levels, especially at 70%, result in increased NOx emissions due to elevated combustion temperatures, despite reducing CO and soot emissions. The study also reveals that the highest thermal efficiency consistently occurs at 25% hydrogen, indicating that moderate hydrogen levels strike the best balance between combustion efficiency and emission control.

At 2000 and 2500 RPM, the maximum combustion efficiency is achieved with 70% hydrogen, but this does not translate to the highest thermal efficiency, which is found at 25%. The elevated temperatures at higher hydrogen levels lead to heat losses and inefficiencies, reducing the overall thermal efficiency. Furthermore, the NOx emissions at 70% hydrogen are significantly higher, while soot emissions are minimized due to hydrogen's cleaner burning properties.

Ultimately, these findings suggest that moderate hydrogen blends, around 25% to 50%, offer the best balance between fuel efficiency and emission control, providing cleaner combustion without the substantial tradeoffs in thermal efficiency and NOx emissions seen at higher hydrogen levels.

8 Future Works

Future research could build upon the findings of this study by addressing several limitations and exploring additional aspects of hydrogen-diesel dual-fuel operation. Firstly, experimental validation under real engine operating conditions should be conducted to verify and complement the simulation results, particularly for combustion characteristics such as ignition delay, in-cylinder pressure traces, and heat release rate. Secondly, future studies could investigate advanced NOx mitigation strategies, such as Exhaust Gas Recirculation (EGR), Selective Catalytic Reduction (SCR), or water injection, and evaluate their combined effect with hydrogen enrichment. Thirdly, optimizing injection timing, pressure, and hydrogen-diesel mixture preparation using multi-objective optimization techniques could further enhance brake thermal efficiency while minimizing emissions. Additionally, expanding the simulation to include transient load conditions, long-term engine durability, and the economic feasibility of hydrogen integration would provide a more comprehensive assessment. Finally, life-cycle analysis of hydrogen production and its supply chain could help determine the overall environmental impact and sustainability of largescale adoption in the transportation sector.

References

- [1] V. Mateichyk et al., "Research of Energy Efficiency and Environmental Performance of Vehicle Power Plant Converted to Work on Alternative Fuels," Machines 2024, Vol. 12, Page 285, vol. 12, no. 5, p. 285, Apr. 2024, doi: 10.3390/MACHINES12050285.
- [2] S. Iliev, "Effects of exhaust gas recirculation (EGR) rates on emission characteristics of ethanol and methanol diesel blended fuels," E3S Web of Conferences, vol. 404, p. 02006, Jul. 2023, doi: 10.1051/E3SCONF/202340402006.
- [3] N. Ghazaly and A. Khodary Emara, "A Review on the Performance Analysis of C.I Engine with Biofuel Blends," SVU-International Journal of Engineering Sciences and Applications, vol. 3, no. 2, pp. 27–36, Dec. 2022, doi: 10.21608/svusrc.2022.128381.1042.
- [4] N. Ghazaly and M. Salah Hofny, "Injection and Combustion of biodiesel at different blends: A review," SVU-International Journal of Engineering Sciences and Applications, vol. 3, no. 2, pp. 37–46, Dec. 2022, doi: 10.21608/svusrc.2022.130956.1043.
- [5] A. Khosravi, "Knock Occurrence Prediction and Performance Optimization of a Natural Gas S.I. Engine," Mapta Journal of Mechanical and Industrial Engineering (MJMIE), vol. 2, no. 3, pp. 1–8, Dec. 2018, doi: 10.33544/MJMIE.V2I3.74.
- [6] S. Santhanakrishnan, "Performance and Emission Characteristics of Al2o3 Coated LHR Engine Operated With Mahua Oil Biodiesel Blend," Int J Res Eng Technol, vol. 02, no. 11, pp. 25–28, Nov. 2013, doi: 10.15623/JJRET.2013.0211004.
- [7] A. Yadav and O. Singh, "Investigations on diesel engine performance based on jatropha, karanja and neem biodiesels," http://dx.doi.org/10.1177/0957650912445016, vol. 226, no. 5, pp. 674–681, Apr. 2012, doi: 10.1177/0957650912445016.
- [8] S. K. Kandasamy and S. K. Kandasamy, "Performance, Combustion, and Emission Characteristics of a VCR Engine Powered by Corn Bio-Diesel," Diesel Engines - Current Challenges and Future Perspectives, Mar. 2024, doi: 10.5772/INTECHOPEN.1002210.
- [9] M. Vijayakumar and P. C. Mukesh Kumar, "Performance and emission characteristics of compression-ignition engine handling biodiesel blends with electronic fumigation," Heliyon, vol. 5, no. 4, p. 1480, Apr. 2019, doi: 10.1016/j.heliyon.2019.e01480.
- [10] Q. Shi, C. H. Zhang, Y. C. Cai, and J. X. Fang, "Effects of Load Ratio on Dual-Fuel Engine Operated with Pilot Diesel Fuel and Liquefied Natural Gas," Adv Mat Res, vol. 960–961, pp. 1389– 1393, 2014, doi: 10.4028/WWW.SCIENTIFIC.NET/AMR.960-961.1389.
- [11] S. M. Mousavi, R. K. Saray, K. Poorghasemi, and A. Maghbouli, "A numerical investigation on combustion and emission characteristics of a dual fuel engine at part load condition," Fuel, vol. 166, pp. 309–319, Feb. 2016, doi: 10.1016/J.FUEL.2015.10.052.
- [12] S. B. Al-Omari, M. Y. E. Selim, and A. A. J. Al-Aseery, "Control of noise and exhaust emissions from dual fuel engines," Journal of Renewable and Sustainable Energy, vol. 3, no. 4, Jul. 2011, doi: 10.1063/1.3596170/284829.
- [13] F. Meng, A. Wijesinghe, J. Colvin, C. Lafleur, and R. Haut, "Conversion of Exhaust Gases from Dual-Fuel (Natural Gas-Diesel) Engine under Ni-Co-Cu/ZSM-5 Catalysts," SAE Technical Papers, vol. 2017-March, no. March, Mar. 2017, doi: 10.4271/2017-01-0908.
- [14] G. Shen, "Design of new clean and efficient combustion mode and thermodynamics research using NSGA-II algorithm," Thermal Science, vol. 24, no. 5 Part A, pp. 2699–2706, 2020, doi: 10.2298/TSCI191016004S.

[15] Moch. A. Kurniawan, D. Yuvenda, and B. Sudarmanta, "The Effects CNG Injection Timing on Engine Performance and Emissions Of A Diesel Dual Fuel Engine," IPTEK The Journal for Technology and Science, vol. 30, no. 2, pp. 64–67, Jul. 2019, doi: 10.12962/J20882033.V30I2.4996.

- [16] C. M. Kumar, P. Rajendra Babu, and A. Professor, "Design & Thermal Analysis of I.C. Engine Poppet Valves using Solidworks and FEA," 2017. [Online]. Available: www.irjet.net
- [17] W. Tutak, A. Jamrozik, and K. Grab-Rogaliński, "Co-Combustion of Hydrogen with Diesel and Biodiesel (RME) in a Dual-Fuel Compression-Ignition Engine," Energies 2023, Vol. 16, Page 4892, vol. 16, no. 13, p. 4892, Jun. 2023, doi: 10.3390/EN16134892.
- [18] D. Akal, S. Öztuna, and M. K. Büyükakın, "A review of hydrogen usage in internal combustion engines (gasoline-Lpgdiesel) from combustion performance aspect," Int J Hydrogen Energy, vol. 45, no. 60, pp. 35257–35268, Dec. 2020, doi: 10.1016/J.IJHYDENE.2020.02.001.
- [19] J. Subramanian, P. Ekambaram, and S. K. Arumugam, "Investigation on combustion and emission characteristics of hydrogen-enriched dual-fuel engine operated under waste frying oil biodiesel," Heat Transfer, vol. 52, no. 2, pp. 1806–1839, Mar. 2023, doi: 10.1002/HTJ.22764.
- [20] S. Jarungthammachote, S. Chuepeng, and P. Chaisermtawan, "Effect of Hydrogen Addition on Diesel Engine Operation and NOx Emission: A Thermodynamic Study," Am J Appl Sci, vol. 9, no. 9, pp. 1472–1478, Aug. 2012, doi: 10.3844/AJASSP.2012.1472.1478.
- [21] N. R. Ammar, "Energy Efficiency and Environmental Analysis of the Green-Hydrogen Fueled Slow Speed Marine Diesel Engine," International Journal of Multidisciplinary and Current Research, vol. Vol.6, no. Nov-Dec-2018, Nov. 2018, doi: 10.14741/IJMCR/V.6.6.10.
- [22] Y. Putrasari et al., "Thermal efficiency and emission characteristics of a diesel-hydrogen dual fuel CI engine at various loads condition," Journal of Mechatronics, Electrical Power, and Vehicular Technology, vol. 9, no. 2, pp. 49–56, Dec. 2018, doi: 10.14203/J.MEV.2018.V9.49-56.
- [23] Y. Karagöz, T. Sandalcl, L. Yüksek, A. S. Dalklllç, and S. Wongwises, "Effect of hydrogen-diesel dual-fuel usage on performance, emissions and diesel combustion in diesel engines," Advances in Mechanical Engineering, vol. 8, no. 8, pp. 1–13, Aug. 2016, doi: 10.1177/1687814016664458/ASSET/IMAGES/LARGE/10.11 77 1687814016664458-FIG7.JPEG.
- [24] B. Li, Y. Chen, F. Zhong, and H. Xu, "Numerical Study on a Diesel/Dissociated Methanol Gas Compression Ignition Engine with Exhaust Gas Recirculation," Applied Sciences 2023, Vol. 13, Page 9612, vol. 13, no. 17, p. 9612, Aug. 2023, doi: 10.3390/APP13179612.
- [25] S. Bhowmik, A. Paul, and R. Panua, "Effect of pilot fuel injection timing on the performance, combustion, and exhaust emissions of biodiesel–ethanol–diethyl ether blend fueled CRDI engine under hydrogen dual fuel strategies," Environ Prog Sustain Energy, vol. 41, no. 4, p. e13784, Jul. 2022, doi: 10.1002/EP.13784.
- [26] R. K. Gopidesi, S. V. Valeti, N. Kumma, A. Mutluri, and B. Venu, "Evaluation dual fuel engine fuelled with hydrogen and biogas as secondary fuel," International Journal of Recent Technology and Engineering, vol. 8, no. 2, pp. 1902–1905, Jul. 2019, doi: 10.35940/ijrte.B1749.078219.
- [27] P. Raju and S. Masimalai, "Numerical Study on a Diesel– Hydrogen Dual-Fuel Engine with Water Injection and Variable Compression Ratio," Energy Technology, vol. 10, no. 7, p. 2100626, Jul. 2022, doi: 10.1002/ENTE.202100626.

- [28] M. M. Ismail, M. Fawzi, F. H. Zulkifli, and S. A. Osman, "Effects of Fuel Ratio on Performance and Emission of Diesel-Compressed Natural Gas (CNG) Dual Fuel Engine," Journal of the Society of Automotive Engineers Malaysia, vol. 2, no. 2, pp. 157–165, Apr. 2018, doi: 10.56381/JSAEM.V2I2.86.
- [29] G. Vidal, T. Yotchou, N. Junior, I. Banta, C. Valery, and N. Abbe, "Experimental Study on the Effect of Load and Air+gas/fuel Ratio on the Performances, Emissions and Combustion Characteristics of Diesel-LPG Fuelled Single Stationary CI Engine," Aug. 2022, doi: 10.21203/RS.3.RS-1871551/V1.
- [30] N. Seelam, S. K. Gugulothu, R. V. Reddy, B. Bhasker, and J. Kumar Panda, "Exploration of engine characteristics in a CRDI diesel engine enriched with hydrogen in dual fuel mode using toroidal combustion chamber," Int J Hydrogen Energy, vol. 47, no. 26, pp. 13157–13167, Mar. 2022, doi: 10.1016/J.IJHYDENE.2022.02.056.
- [31] C. T. Chong and S. Hochgreb, "Measurements of laminar flame speeds of liquid fuels: Jet-A1, diesel, palm methyl esters and blends using particle imaging velocimetry (PIV)," Proceedings of the Combustion Institute, vol. 33, no. 1, pp. 979–986, Jan. 2011, doi: 10.1016/J.PROCI.2010.05.106.
- [32] C. J. Ramsay and K. K. J. R. Dinesh, "Numerical modelling of a heavy-duty diesel-hydrogen dual-fuel engine with late high pressure hydrogen direct injection and diesel pilot," Int J Hydrogen Energy, vol. 49, pp. 674–696, Jan. 2024, doi: 10.1016/J.IJHYDENE.2023.09.019.
- [33] E. Faghani, "Effect of injection strategies on particulate matter emissions from HPDI natural-gas engines.," Vancouver: Ph.D. thesis, The University of British Columbia; 2015.